International Journal on Magnetic Particle Imaging
Vol 9, No 1, Suppl 1, Article ID 2303005, 4 Pages

Infinite Science Publishing

Proceedings Article

System-matrix based reconstruction in magnetic particle imaging.

Alexander Neumann [a,*] · Tobias Klemme [a]

[a] Institute of Medical Engineering, Universität zu Lübeck, Lübeck, Germany
[*] Corresponding author, email: neumann@imt.uni-luebeck.de

Abstract

In this work system-matrix based reconstruction in the context of magnetic particle imaging (MPI) is performed using 2D simulated system matrices and phantoms to study the effects of different approaches in the econstruction chain. As an example, multi color reconstruction at different temperatures is chosen to show how the approach itself changes the reconstruction. It will be shown that a simple and trivial detail has important consequences for the reconstruction algorithms not only halving the number of unknowns but also giving commonly used solvers for the minimization problem a chance to converge to similar solutions.

I. Introduction

Reconstruction is an important step for every imaging technology which uses an indirect measure to obtain information about objects. For the reconstruction an inverse problem must be solved. In the context of magnetic particle imaging (MPI) the indirect measure of the 3D particle concentration is the response of the particles to a spatially dependent magnetic field measured as an induced signal in the receive coils. To go back from the measured signal to the spatial dependent particle concentration the inverse problem needs to be formulated and solved. In MPI there are two dominant reconstruction approaches, x-space reconstruction, and system-matrix based reconstruction. While the former uses a model to describe the particle response and algebraically reconstructs the concentration from the measurement, the latter describes the imaging problem as a system of linear equations using a system matrix, typically obtained by measurement, that contains the information about the particle concentration at each voxel in the field of view under certain physical conditions. An overview of recent developments in the field can be found in [1–3] while a good discussion on different system-matrix based approaches can be found in [4].

II. Material and methods

This work focuses on the basics of system-matrix based reconstructions and evaluates different approaches based on their performance in a 2D multi-color scenario. The data used as phantoms and for the system matrices has been obtained by simulations as described in [5]. The physics of the simulations itself is described in [6] and the implementation can be found on GitHub [7]. The system matrices have a size of 13x13 pixels but only the lower half of it was simulated to shorten the total simulation time. The upper half of the system matrix is obtained by a phase shift of half a period and a sign change in one of the magnetization components [8, 9]. Phantoms and system matrices for different temperatures in the range of 310 −318 K in 2 K steps and a system matrix at 310 K and 326 K have been simulated.
The basic equation for system-matrix based reconstruction is:

$$\mathbf{S}\vec{c} = \vec{u} \tag{1}$$

With $\mathbf{S}$ being the system matrix containing the frequency response of a delta sample at one voxel in each column, $\vec{u}$ being the frequency components of the measured

10.18416/ijmpi.2023.2303005

signal and $\vec{c}$ being the vector of the spatial particle concentration. This work will focus on how eq. 1 can be set up to solve for $\vec{c}$ and what consequences arise for the reconstructed images.

To solve eq. 1 different approaches will be used. The most common one used in MPI is the Kaczmarz method with Tikhonov regularization since it seems to work best. Additionally, this work will also consider singular value decomposition (SVD), as well as the conjugate gradient normal residual (CGNR) method to solve the minimization problem to obtain the desired spatial distribution of concentrations, $\vec{c}$. There are different ways to set up eq. 1 for the different solvers. The most common strategy (A) is as follows [1, 2, 10, 11]: Since $\mathbf{S}$ and $\vec{u}$ are obtained via a fast Fourier transform they are naturally elements of the complex numbers while the wanted concentration vector consists of positive real numbers. The latter is typically enforced by setting $\mathrm{Im}(\vec{c}) = 0$ after one iterative step of the solver. Strategy (B): Here $\mathbf{S}$ is a real matrix by simply splitting the complex numbers in real and imaginary part and appending them or solving the two equations $\mathrm{Re}(\mathbf{S})\vec{c} = \mathrm{Re}(\vec{u}) \wedge \mathrm{Im}(\mathbf{S})\vec{c} = \mathrm{Im}(\vec{u})$ with $\vec{c} \in \mathbb{R}^N$ and N being the number of pixels. In [4], real and imaginary parts are split up for an SVD approach, however, the implications of that strategy have not been discussed. Strategy (A) and Strategy (B) are not equivalent since the solvers for (A) will always look for a solution of the form $\vec{c} = \vec{c}_r + i\vec{c}_i$ which doubles the number of unknowns and could potentially lead to wrong solutions. Consider a problem with two solutions in the imaginary plane. One solution at (-1,1) and another one at (5,0). Applying the above solvers typically returns the solution nearest to the origin, so they would end up finding the (-1,1) solution. Since $\mathrm{Im}(\vec{c})$ is forced to be zero, the final solution will be (-1,0) or (0,0) if positivity ($\vec{c} \geq 0$) is also enforced [12]. However, if the algorithm would have been reformulated to only work with real numbers, the solvers would have found the correct solution of (5,0). In the next section, it will be shown how multi-color reconstruction as proposed in [13] can be influenced by applying the different strategies (A) and (B) for the different solvers.

III. Results and discussion

Fig. 1 shows the multi-color reconstruction results for the different solvers for a phantom at 326 K using strategy (A). As shown, only the Kaczmarz method clearly reconstructs a concentration difference in the different temperature channels. This turns out to be connected to where the constraint of $\mathrm{Im}(\vec{c}) = 0$ is applied within the algorithms. While for SVD - as a direct solving method - the constraint can only be applied on the result, for CGNR and Kaczmarz it can be applied within the iterations. Furthermore, the Kaczmarz method allows the constraint to be applied within one iteration of the matrix itself solving a single row. Moving the constraint in the Kaczmarz method out of this "inner" iteration to the "outer" iteration yields a similar result as the SVD and CGNR approaches showing a lower concentration difference in the two temperature channels. However, for strategy (B) displayed in Fig. 2 it is observed that the difference in the reconstructed concentration channels is independent of the used solvers. All methods yield a similar difference between the two reconstructed channels which is even slightly bigger than the difference reconstructed by the Kaczmarz method using strategy (A) shown in Fig. 1. This indicates that the strategy (A) using the Kaczmarz method has probably not found the optimal solution for a real numbered concentration. To give quantitative results the average and standard deviation for the $c_{310\,\mathrm{K}}/c_{326\,\mathrm{K}}$ phantom pixels and the corresponding background pixels is calculated. Table 1 displays the results for the reconstructions shown Fig. 1 while Table 2 contains the results for Fig. 2

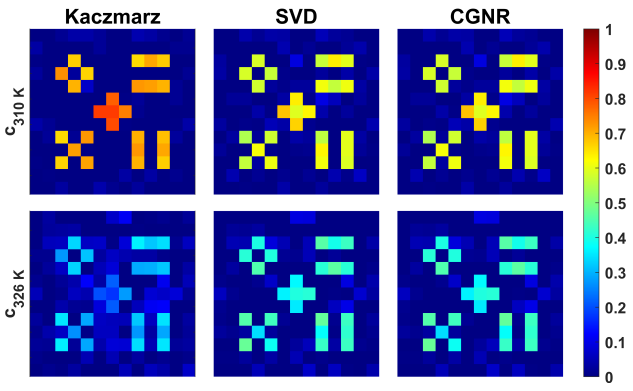

Figure 1: Multi-color reconstruction of a phantom at 310 K using complex numbers for the measured signal and system matrices and forcing $\mathrm{Im}(\vec{c}) = 0$ after an iteration step. The Kaczmarz method can force the restriction while solving single rows of the inverse problem and shows a greater channel difference than the SVD and CGNR method.

Table 1: Average and standard deviation of phantom and background pixels for Fig. 1

	Kaczmarz	SVD	CGNR
phantom $c_{310\,\mathrm{K}}$	0.714 ±0.046	0.599 ±0.034	0.594 ±0.035
phantom $c_{326\,\mathrm{K}}$	0.297 ±0.051	0.415 ±0.036	0.416 ±0.037
background $c_{310\,\mathrm{K}}$	−0.021 ±0.038	−0.002 ±0.035	−0.002 ±0.036
background $c_{326\,\mathrm{K}}$	0.020 ±0.040	−0.002 ±0.039	−0.002 ±0.039

10.18416/ijmpi.2023.2303005

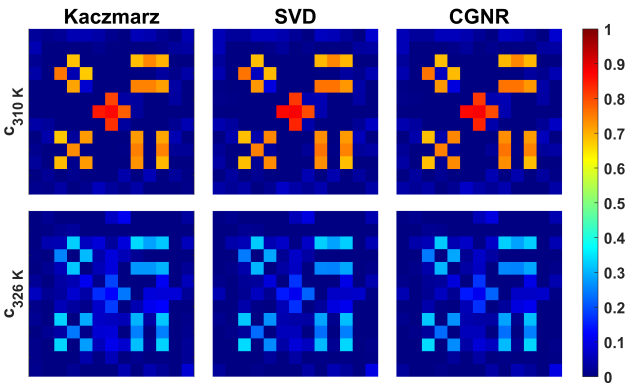

Figure 2: Multi-color reconstruction of a phantom at 310 K using real numbers for the measured signal and system matrices by appending real and imaginary parts. As can be seen, all reconstructions yield a similar result. The observed difference in the channels is slightly higher than for the Kaczmarz method shown in Fig. 1.

Table 2: Average and standard deviation of phantom and background pixels for Fig. 2

	Kaczmarz	SVD	CGNR
phantom $c_{310\,K}$	0.737 ±0.052	0.746 ±0.055	0.746 ±0.055
phantom $c_{326\,K}$	0.274 ±0.057	0.263 ±0.061	0.263 ±0.061
background $c_{310\,K}$	−0.012 ±0.043	−0.002 ±0.041	−0.002 ±0.041
background $c_{326\,K}$	0.014 ±0.045	0.003 ±0.043	0.003 ±0.043

IV. Conclusion

Solving eq. 1 in frequency space using system matrices and signals containing complex numbers (strategy (A)) has been done since the first introduction of MPI in 2005 [10, 12, 14]. From the publications by various authors (e.g. [1–3]) and the available implementations of reconstruction algorithms [11] it seems that the correctness of this approach was not further questioned since it provided plausible and expected results. This work shows that another strategy should be used. Applying or injecting restrictions like $\mathrm{Im}(\vec{c}) = 0$ [10] or $\vec{c} \geq 0$ [12] within/after an iterative step are an improper modification with unknown mathematical consequences. It can result in a plausible solution, as generally observed in MPI, but this shouldn't be taken as proof that the approach is giving the correct solution as demonstrated. Splitting up the signal and system matrices by real and imaginary parts as done in strategy (B) is the mathematical correct way to solve eq. 1 in frequency space with $\vec{c} \in \mathbb{R}^N$. This not only yields the expected result across different solvers, but it is mathematically proven and reduces the number of unknowns by a factor of two. Furthermore, the found behavior for strategy (A) might indicate why the Kaczmarz method is commonly to be believed to work best on MPI datasets.

Additionally, it should be mentioned that eq. 1 can be expressed and solved in the time domain. In this case, system matrices and signals are already real numbers, and no extra care must be taken. However, forcing the restriction $\vec{c} \geq 0$ can also cause similar issue as for $\mathrm{Im}(\vec{c}) = 0$. As such this work proposes to generally avoid forcing artificial mathematical restrictions by setting the solution to fixed values and instead introduce a mathematical expression/penalty term into the optimization/minimization equation representing that restriction or by reformulating the problem itself. For $\mathrm{Im}(\vec{c}) = 0$ this was trivially achieved by splitting the problem in real and imaginary parts. For $\vec{c} \geq 0$ it can be achieved by implementing a logarithmic barrier function into the optimization problem.

Notes

Kaczmarz, SVD and CGNR method used Tikhonov regularization with a regularization value of 10^{-3}. For Kaczmarz and CGNR methods 1000 iterations were used. Signals and system matrices have not been filtered/frequency selected since this is not necessary for simulated data and could be introduced additional uncertainty into the results. To obtain temperatures values out of Fig. 1 and 2 a calibration of the multi-color reconstruction needs to be performed. Since this is not the main topic of this paper that step isn't shown here. For the CGNR method it was observed that it didn't matter if the constrained $\mathrm{Im}(\vec{c}) = 0$ is applied after each iteration or at the end of all iterations. It yielded a similar result in both cases.

Acknowledgments

The authors state no funding involved. The authors thank M. Ahlborg, J. Ackers and J. Schumacher for a discussion around the topic.

Author's statement

Conflict of interest: Authors state no conflict of interest.

References

[1] T. Knopp, N. Gdaniec, and M. Möddel. Magnetic particle imaging: From proof of principle to preclinical applications. *Physics in Medicine & Biology*, 62(14):R124, 2017, doi:10.1088/1361-6560/aa6c99.

[2] L. Yin, W. Li, Y. Du, K. Wang, Z. Liu, H. Hui, and J. Tian. Recent developments of the reconstruction in magnetic particle imaging. *Visual Computing for Industry, Biomedicine, and Art*, 5(1):24, 2022, doi:10.1186/s42492-022-00120-5.

[3] A. Neumann, K. Gräfe, A. von Gladiss, M. Ahlborg, A. Behrends, X. Chen, J. Schumacher, Y. Blancke Soares, T. Friedrich, H. Wei, A. Malhorta, E. Aderhold, A. C. Bakenecker, K. Lüdtke-Buzug, and T. M. Buzug. Recent developments in magnetic particle imaging. *Journal of Magnetism and Magnetic Materials*, 550:169037, 2022, doi:https://doi.org/10.1016/j.jmmm.2022.169037.

[4] T. Kluth and B. Jin. Enhanced reconstruction in magnetic particle imaging by whitening and randomized SVD approximation. *Physics in Medicine & Biology*, 64(12):125026, 2019, doi:10.1088/1361-6560/ab1a4f.

[5] T. Klemme, T. M. Buzug, and A. Neumann. Investigating methods for temperature reconstruction based on simulated data. *International Journal on Magnetic Particle Imaging*, 8(1 Suppl 1), 2022, doi:10.18416/IJMPI.2022.2203059.

[6] A. Neumann and T. M. Buzug. Stochastic simulations of magnetic particles: Comparison of different methods, pp. 213, 2018.

[7] URL: https://github.com/Neumann-A/StochasticPhysics.

[8] A. Weber and T. Knopp, Exploiting the symmetry of the magnetic particle imaging system matrix, in *2013 International Workshop on Magnetic Particle Imaging (IWMPI)*, 1, 2013. doi:10.1109/IWMPI.2013.6528329.

[9] A. Weber and T. Knopp. Symmetries of the 2D magnetic particle imaging system matrix. *Physics in Medicine & Biology*, 60(10):4033, 2015, doi:10.1088/0031-9155/60/10/4033.

[10] J. Weizenecker, J. Borgert, and B. Gleich. A simulation study on the resolution and sensitivity of magnetic particle imaging. *Physics in Medicine & Biology*, 52(21):6363, 2007, doi:10.1088/0031-9155/52/21/001.

[11] T. Knopp, P. Szwargulski, F. Griese, M. Grosser, M. Boberg, and M. Möddel. MPIReco.jl: Julia Package for Image Reconstruction in MPI. *International Journal on Magnetic Particle Imaging*, 5(1-2):1907001, 2019, doi:10.18416/IJMPI.2019.1907001.

[12] J. Weizenecker, B. Gleich, J. Rahmer, H. Dahnke, and J. Borgert. Three-dimensional real-time in vivo magnetic particle imaging. *Physics in Medicine & Biology*, 54(5):L1, 2009, doi:10.1088/0031-9155/54/5/L01.

[13] C. Stehning, B. Gleich, and J. Rahmer. Simultaneous magnetic particle imaging (MPI) and temperature mapping using multi-color MPI. *International Journal on Magnetic Particle Imaging*, 2(2):1612001, 2016, doi:10.18416/ijmpi.2016.1612001.

[14] B. Gleich and J. Weizenecker. Tomographic imaging using the nonlinear response of magnetic particles. *Nature*, 435(7046):1214–1217, 2005, doi:10.1038/nature03808.

